R. & M. No. 3267

MINISTRY OF AVIATION

AERONAUTICAL RESEARCH COUNCIL
REPORTS AND MEMORANDA

The Effect of Temperature Variations in the Plane and Through the Thickness of a Circular Lenticular Plate

By E. H. MANSFIELD, Sc.D., F.R.Ae.S.

LONDON: HER MAJESTY'S STATIONERY OFFICE
1962
SEVEN SHILLINGS NET

The Effect of Temperature Variations in the Plane and Through the Thickness of a Circular Lenticular Plate

By E. H. MANSFIELD, Sc.D., F.R.Ae.S.

COMMUNICATED BY THE DEPUTY CONTROLLER AIRCRAFT (RESEARCH AND DEVELOPMENT), MINISTRY OF AVIATION

*Reports and Memoranda No. 3267**

March, 1961

Summary. This Paper presents a large-deflexion analysis of a thin circular lenticular plate whose temperature varies parabolically in its plane and linearly through its thickness. The analysis embraces the buckled, as well as unbuckled, regimes.

1. *Introduction.* When a wing is subjected to transient heating its temperature will vary from point to point and this will result in the formation of stresses. These 'thermal' stresses may cause a significant loss of torsional and flexural stiffness in a thin solid wing[1, 2, 3] or they may cause buckling of the leading edge[4]. In a built-up wing the thermal stresses will contribute to the buckling of individual panels[5, 6]. In the case of the thin solid wing attention so far has been devoted to the effects of temperature variations in the plane of the wing, but temperature variations through the thickness can also occur due, for example, to solar radiation or to differences in aerodynamic heating of the upper and lower surfaces.

This Report relates to the stresses in and the deflexion of an idealised thin solid wing (hereafter referred to as a plate) which is subjected to certain temperature variations both in its plane and through its thickness. The analysis is based on large-deflexion plate theory[7], but by confining attention to the circular plate of lenticular section it has been possible to obtain exact solutions. Moreover, because of the comparative simplicity of the analysis the investigation has been extended beyond the normal practical range and includes the analysis of the following phenomena: buckling and post-buckling behaviour of the plate subjected to temperature variation in its plane, pre-buckling and post-buckling behaviour with temperature variation through its thickness, and snap-through buckling under combined temperature variations. Finally, consideration is given to the effects of initial curvature in the plate.

* Previously issued as R.A.E. Report No. Structures 268—A.R.C. 22,865.

2. *Some Features of the Circular Lenticular Plate.* The thickness of the plate varies parabolically with r according to the equation

$$\left.\begin{aligned} t &= t_0(1-\rho^2) \\ \rho &= r/r_0, \end{aligned}\right\} \quad \text{where} \tag{1}$$

t_0 is the thickness at the centre and r_0 is the radius of the plate. The rigidity D is therefore given by

$$D = \frac{Et_0^3}{12(1-\nu^2)}(1-\rho^2)^3 \tag{2}$$

where E is Young's modulus and ν is Poisson's ratio.

Two types of temperature distribution are considered. Initially these are considered separately but in Section 5 they are considered in combination. In the first the temperature T is constant across the thickness but varies parabolically in the plane of the plate according to the equation

$$T = T_1\rho^2 + \{Ax + By + C\}. \tag{3}$$

The linear terms in braces do not produce thermal stresses and are henceforth ignored.

The second temperature distribution considered is such that the temperature gradient $\partial T/\partial z$ through the thickness is constant, as is the temperature of the mid-plane of the plate. This temperature distribution would cause each *unrestrained* element of the plate to assume a uniform 'spherical' curvature κ_T such that

$$\kappa_T = -\frac{\partial^2 w}{\partial x^2} = -\frac{\partial^2 w}{\partial y^2} = \alpha\frac{\partial T}{\partial z} = \frac{\alpha T_2}{t_0} \tag{4}$$

where α is the coefficient of thermal expansion and T_2 is the temperature difference across the thickness of the plate at the centre. Any one of the terms κ_T, $\alpha(\partial T/\partial z)$, $\alpha(T_2/t_0)$ may be used to define the magnitude of this temperature distribution, but henceforth only the term κ_T will be used.

Now there are two peculiar features of this lenticular plate which occur when it is subjected to any combination of the two temperature distributions just considered. The first feature is that if the plate deflects it assumes the form

$$w = ar^2\{1 + b\cos 2(\theta - \theta_0)\} \tag{5}$$

where a, b are constants depending on the magnitudes of T_1 and κ_T. The angle θ_0 is arbitrary and there is no loss of generality in assuming it to be 0 or $\frac{1}{2}\pi$. Equation (5) may then be written in the form

$$w = -\tfrac{1}{2}(\kappa_x x^2 + \kappa_y y^2) \tag{6}$$

where κ_x and κ_y are independent of x, y and are the curvatures in the x- and y-directions respectively. It is also convenient to adopt the convention that $\kappa_x \geqslant \kappa_y$, for this can always be achieved by suitable choice of θ_0. For certain ranges of values of T_1 and κ_T the plate deforms with rotational symmetry so that $\kappa_x = \kappa_y$; when this is so we will write

$$w = -\tfrac{1}{2}\kappa r^2. \tag{7}$$

The deflexion of the plate is thus completely determined by the curvatures κ_x, κ_y or κ.

The second feature is that while the magnitude of the middle surface stresses depends on T_1 and κ_T, their *distribution* depends only on the radius r. The middle surface stresses may be derived from a force function Φ according to the relations

$$\left.\begin{aligned} t\sigma_r &= N_r = \frac{1}{r}\frac{\partial \Phi}{\partial r} \\ t\sigma_\theta &= N_\theta = \frac{\partial^2 \Phi}{\partial r^2} \\ \tau_{r\theta} &= 0 \end{aligned}\right\} \tag{8}$$

where

$$\Phi \propto (1-\rho^2)^3 .$$

It will be noticed that Φ varies with r in the same manner as does the rigidity D. Furthermore, the rigidity D has the same dimensions (force $\times$ length) as the force function Φ; because of this it is convenient to write

$$\Phi = \beta D \tag{9}$$

where β is non-dimensional. It follows from Equations (8) and (9) that the entire distribution of middle surface stresses is determined once the value of β is known.

It will be noted that the middle surface stresses are referred to polar co-ordinates. This has been done for reasons of convenience, and because the stresses σ_r, σ_θ are principal stresses. By the same token the stresses due to bending, which will be distinguished by the suffix b, are more conveniently referred to Cartesian co-ordinates. The bending stresses vary linearly through the thickness of the plate and their values on the surface $z = +\frac{1}{2}t$ are given by

$$\left.\begin{aligned} \sigma_{x,b} &= 6M_x/t^2 \\ \sigma_{y,b} &= 6M_y/t^2 \end{aligned}\right\} \tag{10}$$

where the moments per unit length, M_x, M_y are given by

$$\left.\begin{aligned} M_x &= -D\left\{\frac{\partial^2 w}{\partial x^2} + \nu\frac{\partial^2 w}{\partial y^2} + (1+\nu)\kappa_T\right\} \\ M_y &= -D\left\{\frac{\partial^2 w}{\partial y^2} + \nu\frac{\partial^2 w}{\partial x^2} + (1+\nu)\kappa_T\right\}. \end{aligned}\right\} \tag{11}$$

Equations (6), (10) and (11) may be combined to give

$$\left.\begin{aligned} \sigma_{x,b} &= \frac{Et}{2(1-\nu^2)}\{\kappa_x + \nu\kappa_y - (1+\nu)\kappa_T\} \\ \sigma_{y,b} &= \frac{Et}{2(1-\nu^2)}\{\kappa_y + \nu\kappa_x - (1+\nu)\kappa_T\}. \end{aligned}\right\} \tag{12}$$

The maximum value of the bending stresses occurs at the centre where $t = t_0$.

2.1. *Boundary Conditions.* We have already anticipated the forms that Φ and w take, and here it will be shown that these forms satisfy the boundary conditions. In the analyses of Sections 3 to 6, no further mention will be made of the fact that the boundary conditions are satisfied.

There are no forces or moments applied to the edge of the plate so that where $\rho = 1$:

and

$$\left.\begin{aligned} N_r &= N_{r\theta} = 0 \\ M_r &= V_r = 0. \end{aligned}\right\} \tag{13}$$

These conditions are automatically satisfied because the variation of D (and hence Φ) is such that at the edge

$$D = \frac{\partial D}{\partial r} = 0 \tag{14}$$

2.2. *Use of Non-Dimensional Symbols.* The non-dimensional symbols ρ and β have already been introduced. The analysis and presentation of results is also simplified by the introduction of further non-dimensional symbols, which are identified by a circumflex:

$$\left.\begin{aligned} \hat{T} &= \left(\frac{\alpha r_0^2}{t_0^2}\right) T_1 \\ \hat{\kappa}_T &= \left(\frac{\alpha r_0^2}{t_0^2}\right) T_2 \\ &= \left(\frac{r_0^2}{t_0}\right) \kappa_T \\ \{\hat{\kappa},\ \hat{\kappa}_x,\ \hat{\kappa}_y\} &= \left(\frac{r_0^2}{t_0}\right) \{\kappa,\ \kappa_x,\ \kappa_y\} \\ \{\hat{\sigma}_x,\ \hat{\sigma}_y,\ \hat{\sigma}_r,\ \hat{\sigma}_\theta\} &= \left(\frac{r^2{}_0}{Et_0^2}\right) \{\sigma_x,\ \sigma_y,\ \sigma_r,\ \sigma_\theta\}. \end{aligned}\right\} \tag{15}$$

3. *Parabolic Temperature Distribution in Plane of Plate.* For small values of the temperature difference T_1 the plate remains flat but there will be middle surface thermal stresses. For large positive or negative values of T_1 the plate will be buckled and there will be bending stresses in addition to the middle surface stresses. Consider first the thermal stresses prior to buckling.

3.1. *Thermal Stresses Prior to Buckling.* Prior to buckling the force function Φ satisfies the following partial differential equation[7]

$$\nabla^2(\mu\nabla^2\Phi) - (1+\nu)\Diamond^4(\mu,\ \Phi) + E\alpha\nabla^2 T = 0 \tag{16}$$

where

$$\mu = 1/t$$

and

$$\left.\begin{aligned} \Diamond^4(\mu,\ \Phi) &\equiv \frac{\partial^2\mu}{\partial x^2}\frac{\partial^2\Phi}{\partial y^2} - 2\frac{\partial^2\mu}{\partial x\partial y}\frac{\partial^2\Phi}{\partial x\partial y} + \frac{\partial^2\mu}{\partial y^2}\frac{\partial^2\Phi}{\partial x^2} \\ &\equiv \tfrac{1}{2}\{(\nabla^2\mu)(\nabla^2\Phi) + \nabla^2(\mu\nabla^2\Phi + \Phi\nabla^2\mu)\} - \tfrac{1}{4}\{\nabla^4(\mu\Phi) + \mu\nabla^4\Phi + \Phi\nabla^4\mu\}. \end{aligned}\right\}$$

It may be verified that the solution of Equation (16) is given by

$$\beta = \frac{2(1-\nu^2)}{7+\nu}\hat{T} \tag{17}$$

where β is defined by Equation (9).

The middle surface stresses associated with this value of β are given (in non-dimensional form) by

$$\left.\begin{aligned} \hat{\sigma}_r &= \frac{\hat{T}(1-\rho^2)}{7+\nu} \\ \hat{\sigma}_\theta &= \frac{\hat{T}(1-5\rho^2)}{7+\nu}. \end{aligned}\right\} \tag{18}$$

It can be shown that this solution is valid in the range

$$\hat{T}^- \leqslant \hat{T} \leqslant \hat{T}^+$$

where

$$\hat{T}^- = -\frac{7+\nu}{2(1-\nu)} \tag{19}$$
$$\simeq -5{\cdot}21 \quad \text{if} \quad \nu = 0{\cdot}3$$

and

$$\hat{T}^+ = \frac{7+\nu}{2(1+\nu)} \tag{20}$$
$$\simeq 2{\cdot}81.$$

When $\hat{T} < \hat{T}^-$ the temperature at the centre of the plate is so much higher than that at the edge that the plate buckles into a saucer shape. When $\hat{T} > \hat{T}^+$ the temperature at the edge is so much higher than that at the centre that the plate buckles into a saddle shape.

3.2. *Post-Buckling Behaviour.* In the post-buckling phase the force function Φ and the deflexion w satisfy the following simultaneous non-linear partial differential equations[7]:

$$\left.\begin{aligned} \nabla^2(\mu\nabla^2\Phi) - (1+\nu)\Diamond^4(\mu, \Phi) + E\alpha\nabla^2 T + \tfrac{1}{2}E\Diamond^4(w, w) = 0 \\ \text{and} \\ \nabla^2(D\nabla^2 w) - (1-\nu)\Diamond^4(D, w) - \Diamond^4(\Phi, w) = 0. \end{aligned}\right\} \tag{21}$$

3.2.1. *Solution for $\hat{T} < \hat{T}^-$ (hotter at the centre).* It may be verified that the solution of Equations (21) is given by

$$\left.\begin{aligned} \beta &= 1+\nu \\ \text{and} \\ \hat{\kappa} &= \pm 2(\hat{T}^- - \hat{T})^{1/2}. \end{aligned}\right\} \tag{22}$$

The middle surface stresses are thus independent of the temperature and are given by

$$\left.\begin{aligned} \hat{\sigma}_r &= \frac{\rho^2 - 1}{2(1-\nu)} \\ \hat{\sigma}_\theta &= \frac{5\rho^2 - 1}{2(1-\nu)}. \end{aligned}\right\} \tag{23}$$

The bending stresses are given by Equations (12) and (22), whence

$$\hat{\sigma}_{x,b} = \hat{\sigma}_{y\,b} = \pm\left(\frac{1-\rho^2}{1-\nu}\right)(\hat{T}^- - \hat{T})^{1/2}. \tag{24}$$

3.2.2. *Solution for $\hat{T} > \hat{T}^+$ (hotter at the edges).* It may be verified that the solution of Equations (21) is given by

$$\left.\begin{aligned} \beta &= -(1-\nu) \\ \text{and} \\ \hat{\kappa}_x &= -\hat{\kappa}_y = 2(\hat{T} - \hat{T}^+)^{1/2}. \end{aligned}\right\} \tag{25}$$

The middle surface stresses are again independent of the temperature and are given by

$$\left.\begin{aligned} \hat{\sigma}_r &= \frac{1-\rho^2}{2(1+\nu)} \\ \hat{\sigma}_\theta &= \frac{1-5\rho^2}{2(1+\nu)}. \end{aligned}\right\} \tag{26}$$

The bending stresses are given by Equations (12) and (25), whence

$$\hat{\sigma}_{x,b} = -\hat{\sigma}_{y,b} = \left(\frac{1-\rho^2}{1+\nu}\right)(\hat{T}-\hat{T}^+)^{1/2}. \tag{27}$$

The variation with temperature of the principal curvatures, middle-surface stresses and bending stresses has been plotted in Figs. 1 and 2. It is seen there that when $\hat{T} < 1{\cdot}8\hat{T}^-$ or $\hat{T} > 2{\cdot}5\hat{T}^+$ the maximum bending stress exceeds the maximum middle-surface stress.

4. *Linear Temperature Gradient through Thickness of Plate.* When the temperature gradient through the thickness is small the plate deforms into a shallow saucer with constant spherical curvature κ. Initially, when small-deflexion theory is valid, this spherical curvature is equal to κ_T and the plate is free from stress. But this mode of deformation is not a developable surface and accordingly middle-surface stresses are developed as κ increases. These middle-surface stresses 'stiffen' the plate so that the curvature κ becomes less than κ_T and this results in the formation of bending stresses. At a certain critical value of κ_T, denoted here by $\kappa_T{}^*$, the middle-surface stresses assume a dominating rôle and, for $\kappa_T > \kappa_T{}^*$, force the plate into a shape that is no longer rotationally symmetrical. Finally, for $\kappa_T \gg \kappa_T{}^*$ the plate approximates to a developable surface in which the generators are parallel; in other words the plate curls up about a diameter.

The following analysis is based throughout on the large-deflexion plate equations[7]:

$$\left.\begin{aligned} \nabla^2(\mu\nabla^2\Phi) - (1+\nu)\Diamond^4(\mu, \Phi) + \tfrac{1}{2}E\Diamond^4(w, w) &= 0 \\ \text{and} \qquad \nabla^2(D\nabla^2 w) - (1-\nu)\Diamond^4(D, w) + (1+\nu)\nabla^2(D\kappa_T) - \Diamond^4(\Phi, w) &= 0. \end{aligned}\right\} \tag{28}$$

4.1. *Pre-Buckling Behaviour.* It may be verified that the solution of Equations (28) is given by

$$\left.\begin{aligned} \beta &= -\frac{(1-\nu^2)}{2(7+\nu)}\hat{\kappa}^2 \\ \text{where } \hat{\kappa} \text{ is the root of the cubic} \qquad \hat{\kappa}&\left\{1 + \frac{(1-\nu)}{2(7+\nu)}\hat{\kappa}^2\right\} = \hat{\kappa}_T. \end{aligned}\right\} \tag{29}$$

It can also be shown that this solution is valid in the range

$$\left.\begin{aligned} |\hat{\kappa}_T| &\leqslant \hat{\kappa}_T{}^* \\ \text{where} \qquad \hat{\kappa}_T{}^* &= \frac{2}{1+\nu}\left\{\frac{2(7+\nu)}{1+\nu}\right\}^{1/2} \\ &\simeq 5{\cdot}15. \end{aligned}\right\} \tag{30}$$

When $\hat{\kappa}_T = \hat{\kappa}_T{}^*$ the plate is about to buckle and it can be shown that

$$\left.\begin{aligned} \hat{\kappa} &= \hat{\kappa}^*, \text{ say} \\ &= \left\{\frac{2(7+\nu)}{1+\nu}\right\}^{1/2} \\ &\simeq 3{\cdot}35. \end{aligned}\right\} \tag{31}$$

This last result can be written in a dimensional form to express the deflexion at the edge in terms of the thickness t_0, namely

$$\left.\begin{aligned} w_{edge} &= -\tfrac{1}{2}\hat{\kappa}t_0 \\ &\simeq -1{\cdot}67t_0. \end{aligned}\right\} \tag{32}$$

The stresses in the plate during the pre-buckling phase are more conveniently expressed in terms of the curvature symbol $\hat{\kappa}$ rather than $\hat{\kappa}_T$. The middle surface stresses are then given by

$$\left.\begin{aligned}\hat{\sigma}_r &= \frac{1-\rho^2}{2(1+\nu)}\left(\frac{\hat{\kappa}}{\hat{\kappa}^*}\right)^2 \\ \hat{\sigma}_\theta &= \frac{1-5\rho^2}{2(1+\nu)}\left(\frac{\hat{\kappa}}{\hat{\kappa}^*}\right)^2\end{aligned}\right\} \tag{33}$$

and the bending stresses are given by

$$\hat{\sigma}_{x,b} = \hat{\sigma}_{y,b} = -\left(\frac{1-\rho^2}{4(7+\nu)}\right)\hat{\kappa}^3. \tag{34}$$

A point to notice from these equations is that the middle surface stresses vary as the square of the plate curvature, and the bending stresses vary as the cube of the plate curvature. The variation of these stresses with the magnitude of the temperature gradient is more complex because of the non-linear variation of κ with κ_T.

4.2. *Post-Buckling Behaviour.* When $|\hat{\kappa}_T| > \hat{\kappa}_T{}^*$ it may be verified that the solution of Equations (28) is given by

$$\left.\begin{aligned}\beta &= -(1-\nu) \\ \hat{\kappa}_x &= \left(\frac{1+\nu}{2}\right)\{\hat{\kappa}_T + (\hat{\kappa}_T{}^2 - \hat{\kappa}_T{}^{*2})^{1/2}\} \\ \hat{\kappa}_y &= \left(\frac{1+\nu}{2}\right)\{\hat{\kappa}_T - (\hat{\kappa}_T{}^2 - \hat{\kappa}_T{}^{*2})^{1/2}\}.\end{aligned}\right\} \tag{35}$$

The middle surface stresses are thus independent of κ_T and are identical with those discussed in Section 3.2.2 in which $\hat{T} > \hat{T}^+$ (*see* Equation (26)). The bending stresses are given by

$$\left.\begin{aligned}\hat{\sigma}_{x,b} &= -\tfrac{1}{4}(1-\rho^2)\{\hat{\kappa}_T - (\hat{\kappa}_T{}^2 - \hat{\kappa}_T{}^{*2})^{1/2}\} \\ \hat{\sigma}_{y,b} &= -\tfrac{1}{4}(1-\rho^2)\{\hat{\kappa}_T + (\hat{\kappa}_T{}^2 - \hat{\kappa}_T{}^{*2})^{1/2}\}.\end{aligned}\right\} \tag{36}$$

When $|\hat{\kappa}_T| \gg \hat{\kappa}_T{}^*$ Equations (35) and (36) yield the following asymptotic results:

$$\left.\begin{aligned}\hat{\kappa}_x &\to (1+\nu)\hat{\kappa}_T + O\left(\frac{1}{\hat{\kappa}_T}\right) \\ \hat{\kappa}_y &\to 0 + O\left(\frac{1}{\hat{\kappa}_T}\right)\end{aligned}\right\} \tag{37}$$

and

$$\left.\begin{aligned}\hat{\sigma}_{x,b} &\to 0 + O\left(\frac{1}{\hat{\kappa}_T}\right) \\ \hat{\sigma}_{y,b} &\to -\tfrac{1}{2}(1-\rho^2)\hat{\kappa}_T + O\left(\frac{1}{\hat{\kappa}_T}\right).\end{aligned}\right\} \tag{38}$$

These asymptotic results are in accord with *inextensional theory*[8].

The variation with temperature gradient of the principal curvatures, middle surface stresses and bending stresses has been plotted in Figs. 3 and 4.

5. *Temperature Variations in Plane and through Thickness of Plate.* Consider now the behaviour of the plate subjected to an arbitrary combination of the parabolic temperature distribution in the plane of the plate and the linear variation through the thickness. The governing equations are[7]:

$$\left.\begin{aligned}\nabla^2(\mu\nabla^2\Phi) - (1+\nu)\Diamond^4(\mu,\,\Phi) + E\alpha\nabla^2 T + \tfrac{1}{2}E\Diamond^4(w,\,w) = 0\\ \nabla^2(D\nabla^2 w) - (1-\nu)\Diamond^4(D,\,w) + (1+\nu)\nabla^2(D\kappa_T) - \Diamond^4(\Phi,\,w) = 0\end{aligned}\right\} \quad (39)$$

and, as in Sections 3 and 4, it is convenient to consider first the rotationally symmetrical saucer-shaped deflexion.

5.1. *Rotationally Symmetrical Deflexion.* It may be verified that a solution of Equations (39) is given by

$$\beta = -\frac{(1-\nu^2)}{2(7+\nu)}(4\hat{T}+\hat{\kappa}^2) \quad (40)$$

where $\hat{\kappa}$ is a root of the cubic:

$$\hat{\kappa}^3 + 4\hat{\kappa}\left(\hat{T} + \frac{7+\nu}{2(1-\nu)}\right) - \frac{2(7+\nu)}{1-\nu}\hat{\kappa}_T = 0. \quad (41)$$

Equation (41) will have either one or three real roots depending upon the relative magnitudes of $\hat{T}$ and $\hat{\kappa}_T$. It may be shown[9] that there are three real roots if

$$\hat{T} < -\frac{7+\nu}{2(1-\nu)} - \frac{3}{4}\left(\frac{7+\nu}{1-\nu}\right)^{2/3}\hat{\kappa}_T{}^{2/3} \quad (42)$$

and, from physical arguments, the greatest and least roots (algebraically) correspond to stable configurations while the third root corresponds to an unstable configuration; the plate behaves in much the same manner as a bi-metallic strip in a thermostat. Snap-through buckling of the plate will occur if $\hat{\kappa}$ and $\hat{\kappa}_T$ are of opposite sign and

$$\hat{T} = -\frac{7+\nu}{2(1-\nu)} - \frac{3}{4}\left(\frac{7+\nu}{1-\nu}\right)^{2/3}\hat{\kappa}_T{}^{2/3}. \quad (43)$$

During snap-through buckling the curvature $\hat{\kappa}$ jumps from the (unstable) value

$$-\frac{2}{\sqrt{3}}(\hat{T}^- - \hat{T})^{1/2} \text{ to the (stable) value } +\frac{4}{\sqrt{3}}(\hat{T}^- - \hat{T})^{1/2}.$$

It may likewise be shown that there is only one real root of Equation (41) if

$$\hat{T} > -\frac{7+\nu}{2(1-\nu)} - \frac{3}{4}\left(\frac{7+\nu}{1-\nu}\right)^{2/3}\hat{\kappa}_T{}^{2/3} \quad (44)$$

and the corresponding configuration is stable if, in addition,

$$\hat{T} \leqslant \hat{T}^+ - \left(\frac{1+\nu}{4}\right)^2\hat{\kappa}_T{}^2. \quad (45)$$

5.2. *Asymmetrical Deflexion.* It may be verified that if

$$\hat{T} > \hat{T}^+ - \left(\frac{1+\nu}{4}\right)^2\hat{\kappa}_T{}^2 \quad (46)$$

the symmetrical deflexion is unstable and the plate assumes an asymmetrical deflexion in which

$$\beta = -(1-\nu) \quad (47)$$

and

$$\left.\begin{aligned}\hat{\kappa}_x &= \tfrac{1}{2}(1+\nu)\hat{\kappa}_T + \{\tfrac{1}{4}(1+\nu)^2\hat{\kappa}_T{}^2 + 4(\hat{T}-\hat{T}^+)\}^{1/2}\\ \hat{\kappa}_y &= \tfrac{1}{2}(1+\nu)\hat{\kappa}_T - \{\tfrac{1}{4}(1+\nu)^2\hat{\kappa}_T{}^2 + 4(\hat{T}-\hat{T}^+)\}^{1/2}.\end{aligned}\right\} \quad (48)$$

Equations (40), (41), (47) and (48) comprise the complete solution from which the stress distribution and the deflexion may be readily determined for any combination of the two temperature distributions here considered. When the combination of temperature distributions is such that the inequality (42) is satisfied, further information is required as to the 'temperature loading path' in order to distinguish between the two possible stable states.

5.3. *Some Special Cases.* At this point it is convenient to consider some special cases, which are chosen solely because of their interesting features.

5.3.1. *A stress-free plate.* The plate will be free from stress if $\beta = 0$ and $\hat{\kappa} = \hat{\kappa}_T$, and this occurs if

$$4\hat{T} + \hat{\kappa}_T^2 = 0. \tag{49}$$

Equation (49) expresses the fact that the straining of the middle surface, which occurs because it is not a developable surface, is exactly accommodated by the temperature strains in the plane of the plate.

5.3.2. *Plate in which* $\hat{T} = \hat{T}^-$. It is seen from Equation (41) that for such a plate the curvature increases initially as the one third power of $\hat{\kappa}_T$:

$$\hat{\kappa} = \left\{\frac{2(7+\nu)}{1-\nu}\,\hat{\kappa}_T\right\}^{1/3}. \tag{50}$$

Such a rapid variation of curvature is to be expected because the plate is on the point of buckling due to middle surface forces. Equation (50) will be valid only so long as the inequality (45) holds, *i.e.*, until

$$\hat{\kappa}_T = \frac{4}{1+\nu}\left(\frac{7+\nu}{1-\nu^2}\right)^{1/2}$$

beyond which the deflexion will be given by Equation (48).

5.3.3. *Plate in which* $\hat{T} = \hat{T}^+$. Such a plate deflects into a developable surface given by

$$\left.\begin{aligned} \hat{\kappa}_x &= (1+\nu)\hat{\kappa}_T \\ \hat{\kappa}_y &= 0. \end{aligned}\right\} \tag{51}$$

This type of behaviour has been noted previously in an investigation of the flexure and torsion of a heated strip of lenticular section[10].

5.3.4. *Asymptotic behaviour of plate as* $\hat{\kappa}_T$ *and* $\hat{T}$ *increase in proportion.* Suppose that $\hat{T} = \lambda\hat{\kappa}_T$ where λ is a constant. For large values of $\hat{T}$ and $\hat{\kappa}_T$ the deflexion is given by Equation (48):

$$\left.\begin{aligned} \hat{\kappa}_x &= (1+\nu)\hat{\kappa}_T + \frac{4\lambda}{1+\nu} + O\left(\frac{1}{\hat{\kappa}_T}\right) \\ \hat{\kappa}_y &= -\frac{4\lambda}{1+\nu} + O\left(\frac{1}{\hat{\kappa}_T}\right). \end{aligned}\right\} \tag{52}$$

If this expression is compared with Equation (37) it will be seen that the effect of the in-plane temperature distribution is of secondary consideration in determining the deflexion.

6. *Plate with Initial Curvature.* Consider now a circular lenticular plate which has a uniform spherical curvature κ_0 when T and κ_T are zero, and which is initially free from stress. The governing differential equations for a plate with an initial deflexion w_0 are

$$\left.\begin{aligned} \nabla^2(\mu\nabla^2\Phi) - (1+\nu)\Diamond^4(\mu, \Phi) + E\alpha\nabla^2 T + \tfrac{1}{2}E\{\Diamond^4(w, w) - \Diamond^4(w_0, w_0)\} &= 0 \\ \text{and} \qquad \nabla^2\{D\nabla^2(w-w_0)\} - (1-\nu)\Diamond^4(D, w-w_0) + (1+\nu)\nabla^2(D\kappa_T) - \Diamond^4(\Phi, w) &= 0 \end{aligned}\right\} \tag{53}$$

where, in the present instance,

$$w_0 = -\tfrac{1}{2}\kappa_0 r^2 .$$

The solution of Equations (53) may be deduced from the results of the previous Section—and Section 5.3.1 in particular—by noting that, from a purely structural point of view, the stress-free plate with initial curvature κ_0 may be regarded as an initially flat plate in which

$$\left.\begin{aligned} \hat{\kappa}_T &= \hat{\kappa}_0 \\ \text{and} \qquad \hat{T} &= -\tfrac{1}{4}\hat{\kappa}_0^{\,2} . \end{aligned}\right\} \tag{54}$$

It follows that the solution of Equations (53) is given by equations (40), (41), (47) and (48), in which

$$\left.\begin{aligned} \hat{\kappa}_T &\text{ is replaced by } (\hat{\kappa}_T + \hat{\kappa}_0) \\ \text{and} \qquad \hat{T} &\text{ is replaced by } (\hat{T} - \tfrac{1}{4}\hat{\kappa}_0^{\,2}) . \end{aligned}\right\} \tag{55}$$

This solution may be confirmed by substitution. The resulting value of β determines the middle surface stresses, and the curvatures κ, κ_x, κ_y are the actual curvatures of the plate.

6.1. *Rotationally Symmetrical Deflexion.* The equation for determining $\hat{\kappa}$ is:

$$\hat{\kappa}^3 + 4\hat{\kappa}(\hat{T} - \hat{T}^- - \tfrac{1}{4}\hat{\kappa}_0^{\,2}) - \frac{2(7+\nu)}{1-\nu}(\hat{\kappa}_T + \hat{\kappa}_0) = 0 \tag{56}$$

and snap-through buckling occurs when

$$\left(\frac{7+\nu}{1-\nu}\right)^2 (\hat{\kappa}_T + \hat{\kappa}_0)^2 + \frac{64}{27}(\hat{T} - \hat{T}^- - \tfrac{1}{4}\hat{\kappa}_0^{\,2})^3 = 0 . \tag{57}$$

It is interesting to note that if $\hat{\kappa}_T$ and $\hat{T}$ are zero there are two stable states if

$$|\hat{\kappa}_0| \geqslant \hat{\kappa}_0^*$$

where

$$\left.\begin{aligned} \hat{\kappa}_0^* &= 2\left(\frac{2(7+\nu)}{1-\nu}\right)^{1/2} \\ &\doteq 9{\cdot}13 . \end{aligned}\right\} \tag{58}$$

These states are given by

$$\left.\begin{aligned} \hat{\kappa} &= \hat{\kappa}_0 , \\ \text{and} \qquad \hat{\kappa} &= -\tfrac{1}{2}\{\hat{\kappa}_0 + (\hat{\kappa}_0^{\,2} - \hat{\kappa}_0^{*2})^{1/2}\} . \end{aligned}\right\} \tag{59}$$

6.2. *Asymmetrical Deflexion.* The criterion for determining the occurrence of buckling into an asymmetrical mode is given by Equations (46) and (55), which yield

$$16(\hat{T} - \hat{T}^+) = \{(3+\nu)\hat{\kappa}_0 + (1+\nu)\hat{\kappa}_T\}\{(1-\nu)\hat{\kappa}_0 - (1+\nu)\hat{\kappa}_T\} . \tag{60}$$

7. *Example.* The following numerical example is given to indicate the order of magnitude of the buckling phenomena considered in this Paper.

A Duralumin plate, which is initially flat and free from stress, has the following characteristics

$$r_0 = 25 \text{ in.}$$
$$t_0 = 0{\cdot}5 \text{ in.}$$
$$E = 10^7 \text{ lb/sq in.}$$
$$\nu = 0{\cdot}3$$
$$\alpha = 2{\cdot}5 \times 10^{-5}/\text{deg C}.$$

The plate is now heated in such a manner that the temperature in the plane of the plate varies parabolically with r, and is such that the temperature at the centre is 147 deg C higher than that at the edge. Expressed in non-dimensional form this implies that

$$\hat{T} = \left(\frac{\alpha r_0^2}{t_0^2}\right) T_1$$
$$= -9{\cdot}21$$
$$= \hat{T}^- - 4.$$

The plate has therefore buckled into a saucer-like shape whose edge deflexion is given by

$$w_{edge} = \pm \tfrac{1}{2}\hat{\kappa} t_0$$
$$= \pm 1 \text{ in.}$$

From Fig. 3 it will be seen that the middle surface tensile stress σ_0 at the edge is equal to the bending stress at the centre:

$$\sigma = 2{\cdot}86E\left(\frac{t_0}{r_0}\right)^2$$
$$= 11{,}500 \text{ lb/sq in.}$$

It will now be assumed that this parabolic temperature distribution in the plane of the plate is maintained, at $T_1 = -147$ deg C, while the plate is subjected to a linear temperature variation through its thickness. It will also be assumed that κ is initially negative, so that snap-through buckling will occur when, according to Equation (43)

$$\hat{\kappa}_{T,\,snap} = 1{\cdot}19,$$

which corresponds to

$$T_2 = 19 \text{ deg C},$$

at which point w_{edge} jumps from $-0{\cdot}58$ in. to $+1{\cdot}15$ in.

Further increase in T_2 causes the plate to deflect according to Equation (41) until buckling into an asymmetrical mode occurs when

$$\hat{\kappa}_T = 10{\cdot}7,$$

which corresponds to

$$T_2 = 171 \text{ deg C}.$$

The variation of the principal curvatures of the plate over the range $0 < \hat{\kappa}_T < 15$ (corresponding to $0 < T_2 < 240$ deg C) has been plotted in Fig. 5.

8. *Conclusions.* An exact large-deflexion analysis has been presented for a thin circular plate of lenticular section in which the temperature varies parabolically in the plane of the plate and linearly through the thickness. Simple expressions are given for the middle-surface and bending stresses, and for the deflexion. The analysis embraces the buckled, as well as unbuckled states and includes the following novel phenomena: buckling of the plate due to temperature variation through the thickness, and snap-through buckling of a buckled plate due to temperature variations in the plane and through the thickness.

The analysis is extended to include effects of initial curvature.

LIST OF SYMBOLS

(x, y, z)		Cartesian co-ordinates, (x, y) in plane of plate
(r, θ, z)		Cylindrical co-ordinates
r_0		Radius of plate
ρ	$=$	r/r_0
t		Thickness of plate
μ	$=$	$1/t$
D		Flexural rigidity of plate
t_0, D_0		Values of t, D at centre of plate
E		Young's modulus
ν		Poisson's ratio (assumed equal to 0·3 in numerical calculation)
α		Coefficient of thermal expansion
T		Temperature
T_1		Temperature difference in plane of plate, defined by Equation (3)
T_2		Temperature difference through thickness of plate, defined by Equation (4)
κ_T		Curvature defined by Equation (4)
w		Deflexion of plate in z-direction
w_0		Initial deflexion of plate
κ		Uniform spherical curvature of plate
κ_0		Initial curvature of plate
κ_x, κ_y		Curvatures of plate in x- and y-directions
Φ		Force function for plate defined in Equation (8)
$N_r, N_\theta, N_{r\theta}$		Forces per unit length in plane of plate
$\sigma_r, \sigma_\theta, \tau_{r\theta}$ σ_x, σ_y		Stresses in plane of plate
M_x, M_y, M_r		Moments per unit length
V_r		Shear resultant at plate boundary
λ		Constant defined in Section 5.3.4

β	Defined in Equation (9)
∇^2	Laplacian operator
$\Diamond^4$	'Die' operator defined by

$$\Diamond^4(f, g) \equiv \frac{\partial^2 f}{\partial x^2}\frac{\partial^2 g}{\partial y^2} - 2\frac{\partial^2 f}{\partial x \partial y}\frac{\partial^2 g}{\partial x \partial y} + \frac{\partial^2 f}{\partial y^2}\frac{\partial^2 g}{\partial x^2}$$

$$\equiv \tfrac{1}{2}\{(\nabla^2 f)(\nabla^2 g) + \nabla^2(f\nabla^2 g + g\nabla^2 f)\} -$$

$$- \tfrac{1}{4}\{\nabla^4(fg) + f\nabla^4 g + g\nabla^4 f\}$$

Suffix b refers to bending

Circumflex $\hat{}$ denotes non-dimensional symbol defined by Equation (15)

Indices $^-$, $^+$, * refer to critical buckling conditions

REFERENCES

No.	*Author*	*Title, etc.*
1	H. L. Dryden and J. E. Duberg ..	Aero-elastic effects of aerodynamic heating. Paper presented to 5th General Assembly, A.G.A.R.D., Ottawa, Canada. June, 1955.
2	E. H. Mansfield	The influence of aerodynamic heating on the flexural rigidity of a thin wing. A.R.C. R. & M. 3115. September, 1957.
3	S. L. Kochanski and J. H. Argyris	Some effects of kinetic heating on the stiffness of thin wings. Parts I and II. *Aircraft Engineering*. October, 1957 and February, 1958.
4	E. H. Mansfield	Leading edge buckling due to aerodynamic heating. A.R.C. R. & M. 3197. May, 1959.
5	E. W. Parkes	Panels under thermal stress. *Aircraft Engineering*. Vol. XXVIII. No. 328. pp. 180–186. June, 1956.
6	K. I. McKenzie	Leading edge buckling of a thin built-up wing due to aerodynamic heating. A.R.C. 22,982. February, 1961.
7	E. H. Mansfield	On the analysis of elastic plates of variable thickness. *Quart. J. Mech. App. Math.* Vol. XV. Part 2, pp. 167–192, 1962.
8	E. H. Mansfield	The inextensional theory for thin flat plates. *Quart. J. Mech. App. Math.* Vol. VIII. Part 3. pp. 338–352. 1955.
9	H. W. Turnbull	*Theory of equations, University Mathematical Texts*, 5th Edition, 1952. Published by Oliver and Boyd, London.
10	E. H. Mansfield	Combined flexure and torsion of a class of heated thin wings. A.R.C. R. & M. 3195. March, 1958.

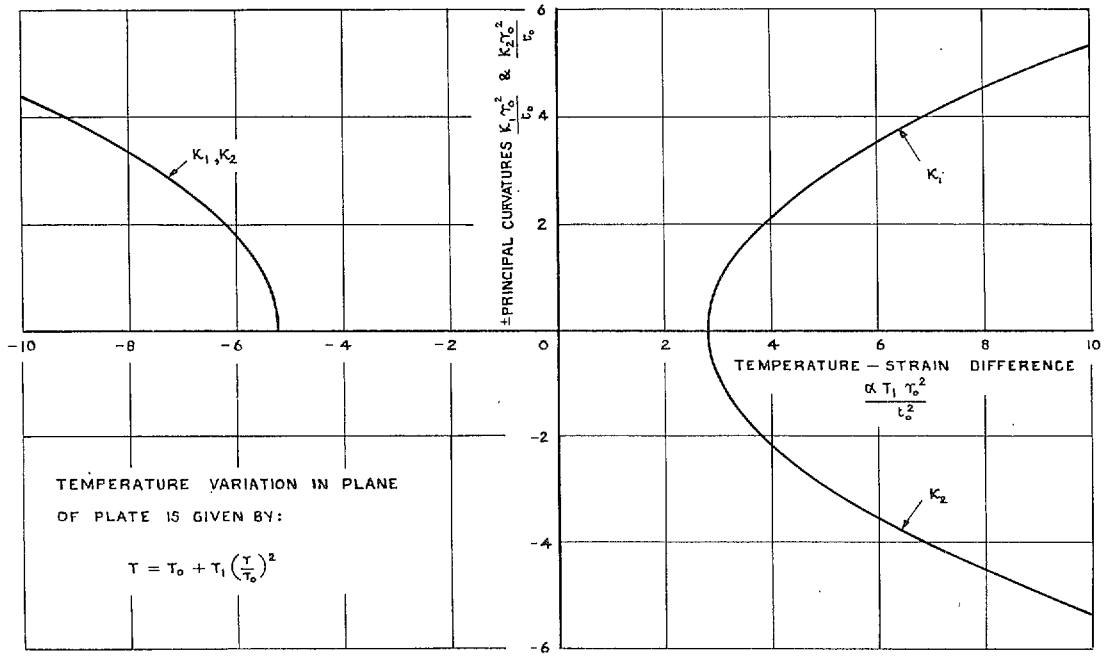

FIG. 1. Variation of principal curvatures with temperature-strain difference in plane of plate.

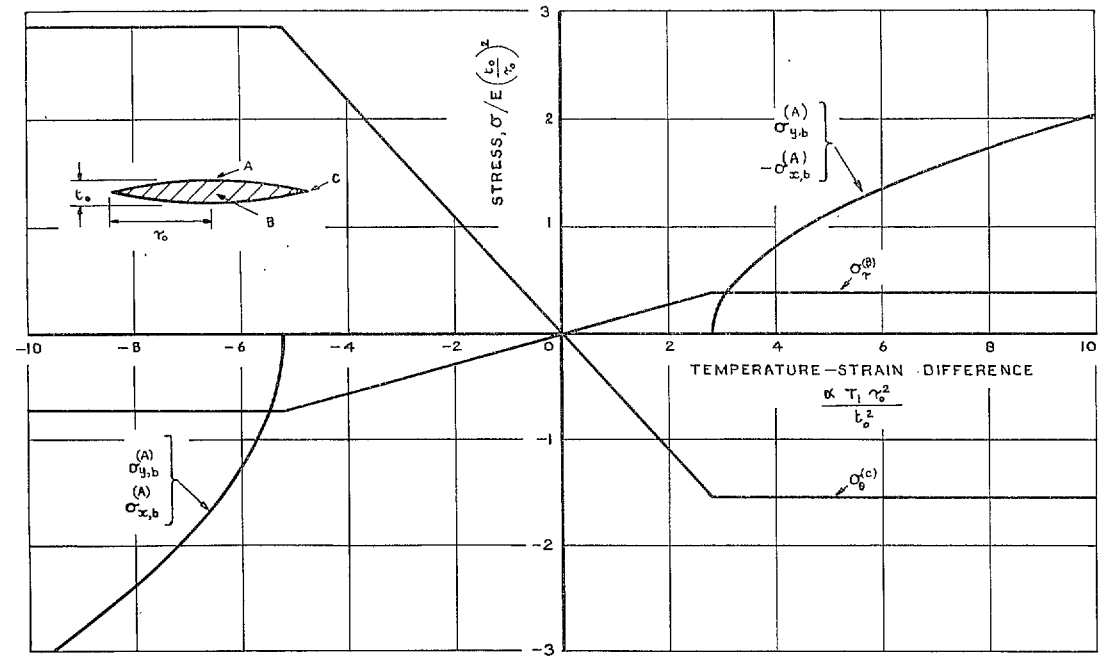

FIG. 2. Variation of middle-surface and bending stresses with temperature-strain difference in plane of plate.

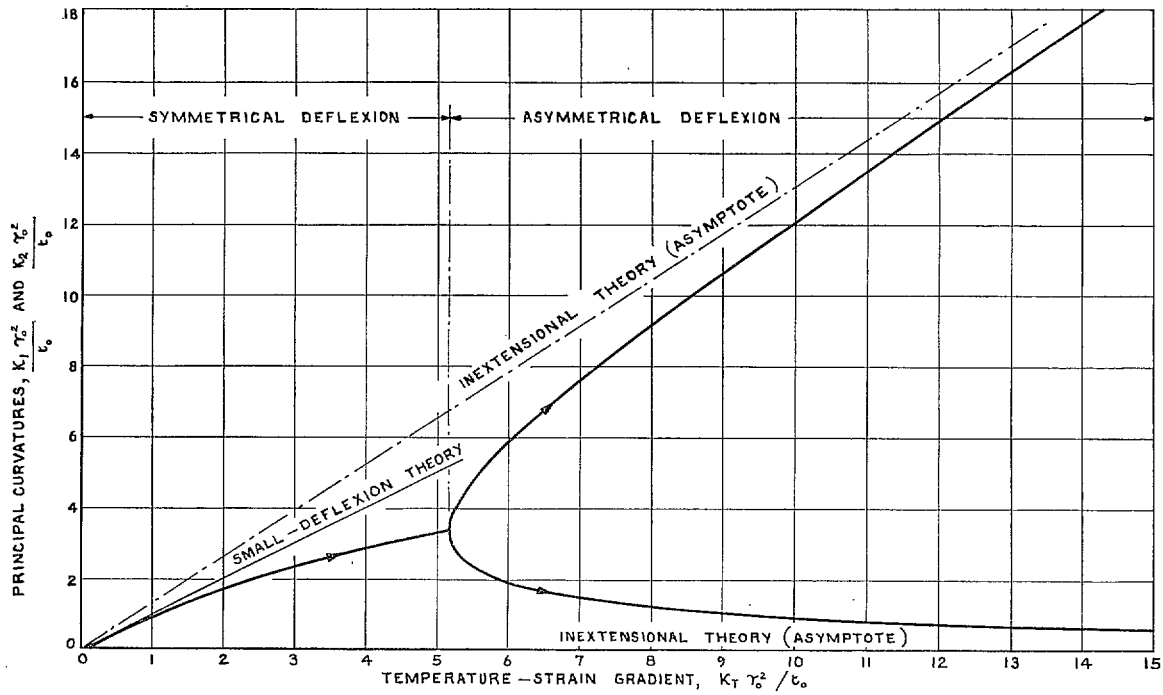

FIG. 3. Variation of principal curvatures with temperature gradient through thickness.

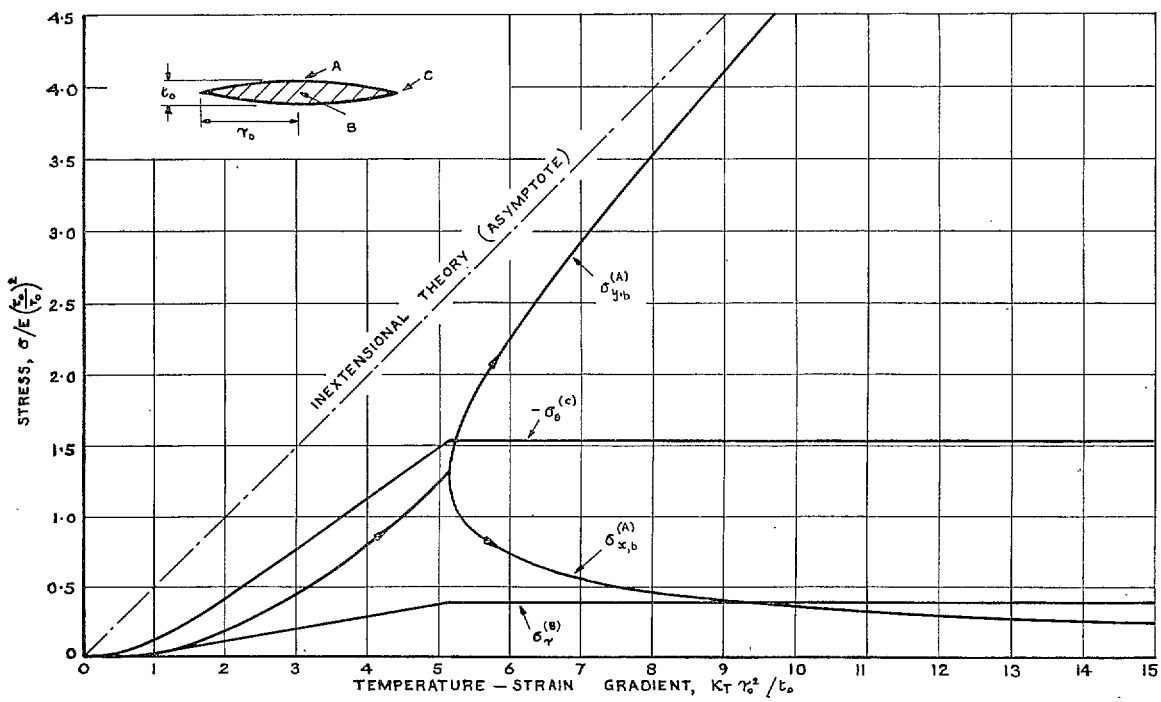

FIG. 4. Variation of middle-surface and bending stresses with temperature gradient through thickness.

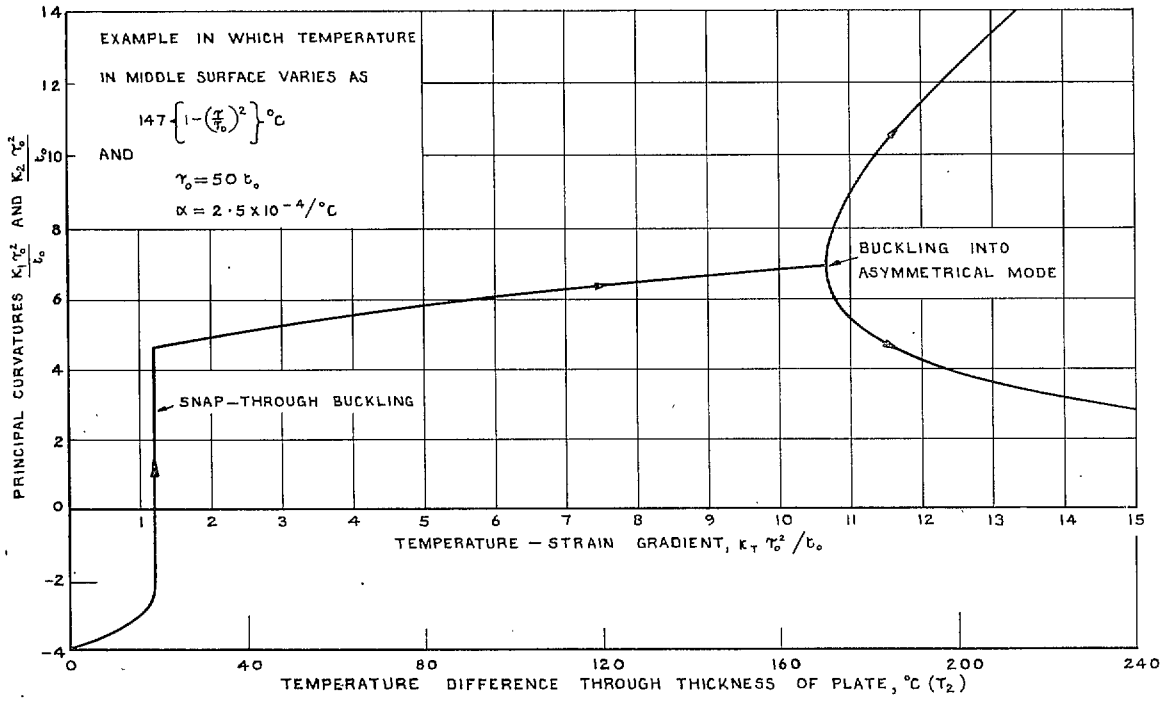

FIG. 5. Variation of principal curvatures with temperature gradient through thickness ($T_1 = -147$ deg C.)

(84218) Wt. 67/1876 K5 6/62 Hw.

Publications of the Aeronautical Research Council

ANNUAL TECHNICAL REPORTS OF THE AERONAUTICAL RESEARCH COUNCIL (BOUND VOLUMES)

1942 Vol. I. Aero and Hydrodynamics, Aerofoils, Airscrews, Engines. 75*s.* (post 2*s.* 9*d.*)
Vol. II. Noise, Parachutes, Stability and Control, Structures, Vibration, Wind Tunnels. 47*s.* 6*d.* (post 2*s.* 3*d.*)

1943 Vol. I. Aerodynamics, Aerofoils, Airscrews. 80*s.* (post 2*s.* 6*d.*)
Vol. II. Engines, Flutter, Materials, Parachutes, Performance, Stability and Control, Structures. 90*s.* (post 2*s.* 9*d.*)

1944 Vol. I. Aero and Hydrodynamics, Aerofoils, Aircraft, Airscrews, Controls. 84*s.* (post 3*s.*)
Vol. II. Flutter and Vibration, Materials, Miscellaneous, Navigation, Parachutes, Performance, Plates and Panels, Stability, Structures, Test Equipment, Wind Tunnels. 84*s.* (post 3*s.*)

1945 Vol. I. Aero and Hydrodynamics, Aerofoils. 130*s.* (post 3*s.* 6*d.*)
Vol. II. Aircraft, Airscrews, Controls. 130*s.* (post 3*s.* 6*d.*)
Vol. III. Flutter and Vibration, Instruments, Miscellaneous, Parachutes, Plates and Panels, Propulsion. 130*s.* (post 3*s.* 3*d.*)
Vol. IV. Stability, Structures, Wind Tunnels, Wind Tunnel Technique. 130*s.* (post 3*s.* 3*d.*)

1946 Vol. I. Accidents, Aerodynamics, Aerofoils and Hydrofoils. 168*s.* (post 3*s.* 9*d.*)
Vol. II. Airscrews, Cabin Cooling, Chemical Hazards, Controls, Flames, Flutter, Helicopters, Instruments and Instrumentation, Interference, Jets, Miscellaneous, Parachutes. 168*s.* (post 3*s.* 3*d.*)
Vol. III. Performance, Propulsion, Seaplanes, Stability, Structures, Wind Tunnels. 168*s.* (post 3*s.* 6*d.*)

1947 Vol. I. Aerodynamics, Aerofoils, Aircraft. 168*s.* (post 3*s.* 9*d.*)
Vol. II. Airscrews and Rotors, Controls, Flutter, Materials, Miscellaneous, Parachutes, Propulsion, Seaplanes, Stability, Structures, Take-off and Landing. 168*s.* (post 3*s.* 9*d.*)

1948 Vol. I. Aerodynamics, Aerofoils, Aircraft, Airscrews, Controls, Flutter and Vibration, Helicopters, Instruments, Propulsion, Seaplane, Stability, Structures, Wind Tunnels. 130*s.* (post 3*s.* 3*d.*)
Vol. II. Aerodynamics, Aerofoils, Aircraft, Airscrews, Controls, Flutter and Vibration, Helicopters, Instruments, Propulsion, Seaplane, Stability, Structures, Wind Tunnels. 110*s.* (post 3*s.* 3*d.*)

Special Volumes

Vol. I. Aero and Hydrodynamics, Aerofoils, Controls, Flutter, Kites, Parachutes, Performance, Propulsion, Stability. 126*s.* (post 3*s.*)
Vol. II. Aero and Hydrodynamics, Aerofoils, Airscrews, Controls, Flutter, Materials, Miscellaneous, Parachutes, Propulsion, Stability, Structures. 147*s.* (post 3*s.*)
Vol. III. Aero and Hydrodynamics, Aerofoils, Airscrews, Controls, Flutter, Kites, Miscellaneous, Parachutes, Propulsion, Seaplanes, Stability, Structures, Test Equipment. 189*s.* (post 3*s.* 9*d.*)

Reviews of the Aeronautical Research Council

1939–48 3*s.* (post 6*d.*) 1949–54 5*s.* (post 5*d.*)

Index to all Reports and Memoranda published in the Annual Technical Reports

1909–1947 R. & M. 2600 (out of print)

Indexes to the Reports and Memoranda of the Aeronautical Research Council

Between Nos. 2351–2449	R. & M. No. 2450 2*s.* (post 3*d.*)
Between Nos. 2451–2549	R. & M. No. 2550 2*s.* 6*d.* (post 3*d.*)
Between Nos. 2551–2649	R. & M. No. 2650 2*s.* 6*d.* (post 3*d.*)
Between Nos. 2651–2749	R. & M. No. 2750 2*s.* 6*d.* (post 3*d.*)
Between Nos. 2751–2849	R. & M. No. 2850 2*s.* 6*d.* (post 3*d.*)
Between Nos. 2851–2949	R. & M. No. 2950 3*s.* (post 3*d.*)
Between Nos. 2951–3049	R. & M. No. 3050 3*s.* 6*d.* (post 3*d.*)
Between Nos. 3051–3149	R. & M. No. 3150 3*s.* 6*d.* (post 3*d.*)

HER MAJESTY'S STATIONERY OFFICE

from the addresses overleaf

Printed and published by
HER MAJESTY'S STATIONERY OFFICE

To be purchased from
York House, Kingsway, London W.C.2
423 Oxford Street, London W.1
13A Castle Street, Edinburgh 2
109 St. Mary Street, Cardiff
39 King Street, Manchester 2
50 Fairfax Street, Bristol 1
35 Smallbrook, Ringway, Birmingham 5
80 Chichester Street, Belfast 1
or through any bookseller

Printed in England

S.O. Code No. 23-3267